NC100668, A NEW TRACER FOR IMAGING OF VENOUS THROMBOEMBOLISM: DISPOSITION AND METABOLISM IN RATS

Tore Skotland, Svein Olaf Hustvedt, Inger Oulie, Petter Balke Jacobsen, Grete Arneberg Friisk, Ann Svendsen Langøy, Steinar Uran, Jessie Sandosham, Alan Cuthbertson, and Kim Gunnar Toft

Research and Development, GE Healthcare Bio-Sciences, Oslo, Norway

ABSTRACT:

The ^{99m}Tc-complex of NC100668 [Acetyl-Asn-Gln-Glu-Gln-Val-Ser-Pro-Tyr(3-iodo)-Thr-Leu-Leu-Lys-Gly-NC100194] is being evaluated for nuclear medical imaging of venous thromboembolism. NC100668 is a 13-amino acid peptide with a Tc-binding chelator [NC100194; -NH-CH$_2$-CH$_2$-N(CH$_2$-CH$_2$-NH-C(CH$_3$)$_2$-C(CH$_3$)=N-OH)$_2$] linked to the C-terminal end. Following injection in rats of [Asn-U-^{14}C]NC100668 (labeling of the N-terminal amino acid), approximately 70% of the radioactivity was recovered in urine within 3 days. Following injection of [Lys-U-^{14}C]NC100668 (labeling close to the C-terminal amino acid), radioactivity was cleared more slowly, with only 8% recovered in urine and approximately 80% of the radioactivity present in the body after 3 days. The highest concentration of radioactivity in the body following injection of [Lys-U-^{14}C]NC100668 was observed in the kidney inner cortex; this probably represents ^{14}C-labeled Lys, which is reabsorbed in the kidney tubules and incorporated into protein metabolism. Metabolite profiling by high-performance liquid chromatography with radiochemical detection revealed that following injection of [Asn-U-^{14}C]NC100668, there is a rapid appearance in blood of one peak containing radioactive metabolite(s) originating from the N-terminal part of the molecule. In urine samples, only this radioactive peak was observed with no intact NC100668 remaining; this very hydrophilic N-terminal metabolite was probably either the N-terminal amino acid or a very short peptide. Liquid chromatography-mass spectrometry analyses of rat urine samples obtained after injection of nonlabeled NC100668 confirmed the identity of two metabolites generated from the C-terminal end of the molecule; Gly-NC100194 was identified as the major of these metabolites and NC100194 as a minor metabolite present at approximately one-tenth the amount of Gly-NC100194. No other metabolites were identified.

NC100668 consists of a 13-amino acid peptide, N-terminally blocked with an acetyl group containing an iodinated tyrosine and coupled to a Tc-chelator (NC100194) via the C-terminal glycine. Using the common three-letter abbreviations for amino acids, the structure of NC100668 is Acetyl-Asn-Gln-Glu-Gln-Val-Ser-Pro-Tyr(3-iodo)-Thr-Leu-Leu-Lys-Gly-NC100194, where NC100194 is represented by the chemical formula -NH-CH$_2$-CH$_2$-N(CH$_2$-CH$_2$-NH-C(CH$_3$)$_2$-C(CH$_3$)=N-OH)$_2$. The detailed structure is shown in Fig. 1.

^{99m}Tc-NC100668 is being developed as a diagnostic radiopharmaceutical for imaging of venous thromboembolism, which is a major health problem with an estimated average annual incidence in the United States exceeding 1 per 1000 (Silverstein et al., 1998). The peptide moiety of NC100668 is similar to part of the N-terminal sequence in α_2-antiplasmin (Moroi and Aoki, 1976; Lijnen et al., 1987). The mechanism of action is by covalent linking between a glutamine in α_2-antiplasmin (corresponding to Gln-2 in NC100668) and a lysine in fibrin mediated by enzymatic action of blood coagulation factor XIIIa (Ichinose et al., 1983; Lee et al., 2001; Jaffer et al., 2004).

Diagnostic radiopharmaceuticals are radioactive substances that are administered to patients. Many of these agents are labeled with the γ-emitter ^{99m}Tc, which has a half-life of 6.02 h (Liu et al., 1997). Due to the short half-life, the ^{99m}Tc-based agents are distributed to hospitals in a Tc-free form as a freeze-dried product ready for labeling with technetium. On the day of the imaging procedure, the ^{99m}Tc is added to the product as the pertechnetate anion TcO$_4^-$ eluted from a ^{99}Mo/^{99m}Tc generator with saline. The freeze-dried substances are then solubilized in saline in the presence of a reducing agent, which converts the pertechnetate to a lower oxidation state, facilitating coordination to the chelate component of the agent. There is a vast excess of the agent compared with the added Tc as typically less than 1% of the injected agent is in the form of the Tc complex. Hence, the unlabeled agent makes up almost the entire amount of the chemical entity injected, whereas there is only the very small amount of the ^{99m}Tc-labeled agent, which is visualized during the diagnostic imaging procedure. The Tc-free substance is therefore in focus when
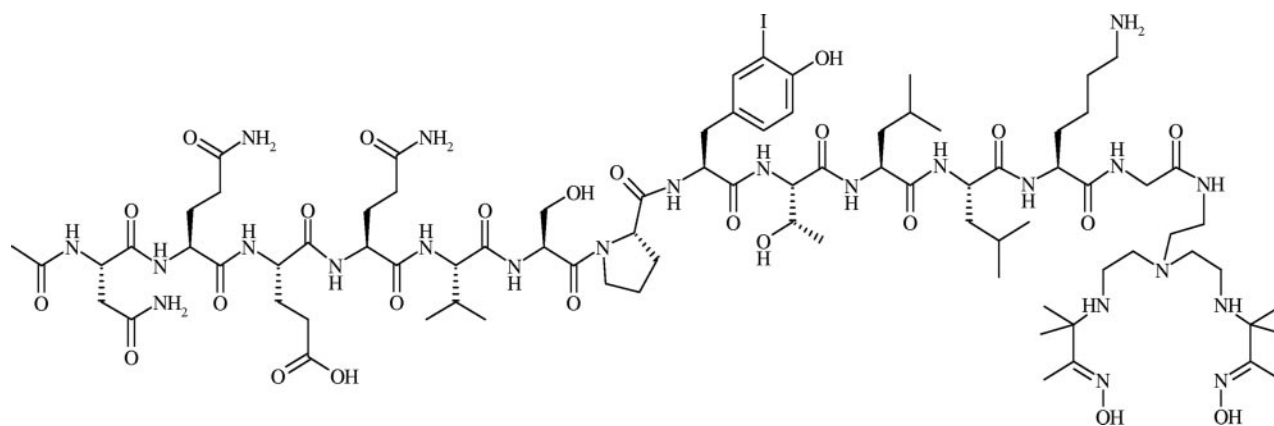
Fig. 1. The molecular structure of NC100668.

describing metabolism and evaluating safety of such agents; the human dose of NC100668 is less than 100 μg.

The present study was set up to study the disposition and metabolism of NC100668. The main focus has been on data obtained following intravenous injection of NC100668 to rats, but results of in vitro experiments performed with rat and human blood are also included. In this study, three different substances were used, i.e., unlabeled NC100668 and two different ^{14}C-labeled analogs of NC100668. The ^{14}C labeling was either in the N-terminal amino acid Asn or in the Lys residue close to the C-terminal end, i.e., close to the ^{99m}Tc-binding chelator NC100194. This report also includes discussions regarding the enzymes most likely to be involved in the metabolism of NC100668.

Materials and Methods

Reagents and Substances. NC100194 (chelate) was supplied by GE Healthcare (Oslo, Norway). [Asn-U-^{14}C]NC100668 (7.77 GBq/mmol; radiochemical purity, 95%) and [Lys-U-^{14}C]NC100668 (13.0 GBq/mmol; radiochemical purity, 93%) were from GE Healthcare (Cardiff, UK). Carboxymethylcellulose sodium, low viscosity, was obtained from Norsk Medisinaldepot, Oslo, Norway. All amino acids were in the L-form and purchased from Novabiochem (Läufelfingen, Switzerland); Fmoc-Tyr(3-iodo)-OH was purchased from Bachem AG (Bubendorf, Switzerland). The protease inhibitor cocktail used was P8340 from Sigma-Aldrich (St. Louis, MO). All other chemicals were of analytical grade quality. Water was purified by reversed osmosis, ion-exchanged, and filtered through a 0.45-μm filter on a Milli-Q Reagent Water System (Millipore, Molsheim, France).

Synthesis of NC100668, Gly-NC100194, and Three Short Peptides. The peptide H-Asn(trityl)-Gln(trityl)-Glu(tertiary butyl ester)-Gln(trityl)-Val-Ser-(tertiary butyl)-Pro-Tyr(2-iodo)-Thr(tertiary butyl)-Leu-Leu-Lys(Boc)-Gly was assembled on SASRIN resin (super acid-sensitive resin; Bachem AG) using an Applied Biosystems 433A peptide synthesizer (Applied Biosystems, Foster City, CA) and Fmoc chemistry starting with 0.3 mmol SASRIN resin. An excess of 1 mmol preactivated amino acids, activated with O-benzotriazol-1-yl-N,N,N',N'-tetramethyluronium hexafluorophosphate, was applied in the coupling steps. The N terminus was acetylated using a solution of 1.2 mmol acetic acid, 1.2 mmol PyBOP, 1.2 mmol hydroxybenzotriazole, and 2.4 mmol N-methylmorpholine in DMF for 60 min. Following cleavage of the still side chain-protected peptide from the SASRIN resin in 0.1% TFA, the peptide was activated in DMF with PyBOP and reacted with 1.2 Eq of the chelate (NC100194). The reaction was stirred for 16 h after which the DMF was removed in vacuo. All remaining protecting groups were removed in TFA containing 2.5% triisopropylsilane and 2.5% water. The crude peptide residue, following evaporation of solvent, was reconstituted in a water/acetonitrile mixture and purified by preparative HPLC on a Phenomenex Luna column (Phenomenex, Torrance, CA).

Gly-NC100194 was prepared from Boc-Gly activated with PyBOP (as above) followed by addition of 1.2 Eq of NC100194 in DMF (3 h). The

product was liberated following evaporation of DMF, removal of the Boc group with TFA, and HPLC purification of the crude material in good yield.

Acetyl-Asn-Gln, Val-Ser-Pro-Tyr and Val-Ser-Pro-Tyr(3-iodo) were synthesized using standard Fmoc chemistry and the Applied Biosystems 433A synthesizer. All synthesized substances were characterized by MS and shown by HPLC analyses to have a purity of greater than 98%.

Quantitative Whole-Body Autoradiography (QWBA). The rats used were outbred male BrlWistHam@Mol obtained from Harlan, Bicester, UK and weighed 180 to 240 g at time of injection. They were randomly allocated to polycarbonate cages type III-1290 (three per cage), identified by numbered ear tags, and allowed 1 week of acclimatization before the start of the study. The temperature was kept at 21 ± 2°C, and the humidity was maintained at 55 ± 10%. Lighting was controlled to give 12 h light and 12 h dark in phase with normal daylight. The rats were provided municipally supplied tap water and diet (Rat and Mouse 1 Maintenance Diet; Special Diets Service, Northwich, UK) ad libitum. All animal experiments complied with legal requirements and internal guidelines.

Eight male rats and three female rats were injected with each of the two radiolabeled substances in the quantitative whole-body autoradiography experiments. Rats injected with [Asn-U-^{14}C]NC100668 received a dose of 389 kBq/kg equivalent to a NC100668 dose of 559 μg/kg, whereas the rats injected with [Lys-U-^{14}C]NC100668 received 600 kBq/kg equivalent to a NC100668 dose of 516 μg/kg. All animals were given deep surgical anesthesia by inhalation of isofluran before they were euthanized using liquid N_2, and the carcasses were stored in a −20°C freezer until prepared for QWBA analysis. For each substance, one male rat was euthanized at each of the following time points: 5 min, 20 min, 1 h, 4 h, 7 h, 24 h, 3 days, and 7 days postdosing, whereas the female rats were euthanized at 5 min, 1 h, and 24 h.

The rats were prepared for the QWBA analyses after a modified method as described by Ullberg (1977). Briefly, rats were embedded in aqueous carboxymethylcellulose, 2% (w/v), by immersion in a hexane/dry ice bath (−70°C) for approximately 30 min. The microtome stage and embedding frame (Leica, Wetzlar, Germany) were precooled in the freezing mixture. The animal blocks were placed into appropriately labeled bags with unique identification and stored in a −20°C freezer until sectioning. Appropriate sections with a thickness of 25 μm were collected on adhesive tape (Scotch Brand 821; 3M, St. Paul, MN) using a Leica cryomicrotome CM 3600 with a temperature at approximately −20°C. The sections were dehydrated overnight and placed against imaging plates (FUJI BAS III Imaging Plates; Fuji Photo Film Ltd., Tokyo, Japan). The imaging plates for whole-body sections were exposed for 7 days, whereas imaging plates with sections through the kidney section were exposed for 3 days to avoid overexposure. The imaging plates were scanned using a FUJIFILM BioImager Analyzer BAS-2500 with BASReader software version 2.21 (Fuji Photo Film Ltd.), and the resulting images were imported into AIDA software version 3.10 (raytest, Straubenhardt, Germany) for quantification. All visible organs listed in Tables 1 and 2 (and not exhibiting overexposure) were measured. The results were compared with calibration standards, which were sectioned, exposed, and measured as described above, containing from 0.3 kBq/g to 75 kBq/g of each of the ^{14}C-labeled test items.

TABLE 1

QWBA data and excretion data following injection of [Asn-U-^{14}C]NC100668 in male rats

Data for all organs are given as micrograms of equivalent per gram, i.e. the data are corrected with the self-absorption coefficients. The recoveries from urine and feces as well as the calculated recoveries for the whole-body and the total recovery are given as %ID. N.P., not present in the images. The data collected for urine during the first period (0–6 h) are shown together with the data for the animal killed 7 h after dosing.

	5 Min	20 Min	1 H	4 H	7 H	24 H	3 Days	7 Days
Adrenal	0.54	0.37	0.31	0.27	0.26	0.31	0.16	0.09
Blood	0.97	0.62	0.14	0.08	0.10	0.07	0.08	0.06
Bone marrow	0.41	0.31	0.45	0.35	0.34	0.39	0.16	0.06
Bone mineral	0.08	0.11	0.04	0.02	0.04	0.05	0.03	0.03
Brain	0.01	0.01	0.02	0.01	0.01	0.01	0.01	0.02
Epididymis	0.32	0.44	0.22	0.12	0.11	0.12	0.05	0.05
Eye	0.10	0.05	0.10	0.02	0.02	0.03	0.03	0.04
Fat (brown)	0.40	N.P.	0.10	N.P.	0.13	N.P.	N.P.	0.07
Fat (white)	0.16	0.07	0.04	0.02	0.03	0.02	0.04	0.04
Harderian gland	0.27	0.13	0.15	0.09	0.08	0.11	0.08	0.06
Heart muscle	0.53	0.35	0.13	0.10	0.09	0.09	0.09	0.08
Intestine (small)	0.31	0.26	0.30	0.41	0.31	0.38	0.11	0.05
Intestine (large)	0.37	0.18	0.22	0.18	0.21	0.16	0.15	0.06
Kidney	6.54	8.60	3.69	1.35	1.07	0.94	0.76	0.24
Liver	0.92	0.80	0.52	0.31	0.27	0.24	0.18	0.09
Lung	0.60	0.44	0.20	0.10	0.10	0.11	0.09	0.07
Muscle	0.19	0.18	0.09	0.07	0.07	0.08	0.10	0.07
Pancreas	0.35	0.46	1.92	0.36	0.36	0.14	0.09	0.06
Testes	0.11	0.20	0.10	0.04	0.04	0.05	0.04	0.04
Salivary gland	0.38	0.31	0.36	0.46	0.34	0.16	0.11	0.06
Seminal vesicles	0.03	0.02	0.02	0.14	0.12	0.23	0.15	0.08
Skin	0.34	0.55	0.18	0.08	0.09	0.10	0.11	0.08
Spinal cord	0.02	0.02	0.02	0.02	0.01	0.02	0.02	0.03
Spleen	0.42	0.45	0.63	0.28	0.32	0.25	0.17	0.09
Stomach	0.35	0.34	0.52	0.29	0.28	0.23	0.11	0.07
Stomach content	0.00	0.01	0.00	0.54	0.08	0.00	0.00	0.02
Thymus	0.21	0.12	0.15	0.16	0.16	0.18	0.16	0.07
Urine bladder	0.10	18.00	17.2	0.35	0.77	0.02	0.03	0.04
Prostate	0.31	0.18	0.13	0.12	0.12	0.23	0.10	0.05
Recovery QWBA	81.2	91.0	45.4	20.2	22.5	18.7	17.4	13.4
Urine (mean ± S.D.; $n = 3$)					62.0 ± 6.6	69.9 ± 1.1	70.5 ± 1.1	70.9 ± 1.1
Feces (mean ± S.D.; $n = 3$)						1.0 ± 0.8	1.8 ± 1.2	2.1 ± 1.3
Total recovery					84.5	89.6	89.6	86.5

All data given are based on signal intensity values within a range giving a reproducibility of the standard samples better than ± 8%. The following self-absorption coefficients (SAC) were used to calculate micrograms of equivalent per gram according to an internal validation report (μg Eq/g$_{(reported)}$ = μg Eq/g$_{(measured)}$ · SAC): bone mineral, 1.50; eye, 1.24; brown fat, 1.19; white fat, 1.43; skin, 1.14; and all other organs, 1.0. The following weighting factors (WF) were used to calculate the %ID per organ (%ID = μg Eq/g$_{(reported)}$ · WF · body weight · 100/dose): blood, 0.058; brain 0.009; white fat, 0.07; intestine (small), 0.029; intestine (large), 0.024; kidney, 0.012; liver, 0.049; lung, 0.012; muscle, 0.43; skin, 0.18; and all other organs, adding up to 0.13.

Radiochemical Quantification of Urine and Fecal Samples. To measure the radioactivity excreted in urine and feces, a total of three male rats were injected with each of the two ^{14}C-labeled substances and placed in metabolism cages for 7 days (handling and dosing as described above for the QWBA study; one of these rats was used for the QWBA study). Urine samples were collected at the following intervals: 0 to 6 h, 6 to 24 h, and then 24 h intervals up to 7 days. Feces were sampled at 24-h intervals for 7 days.

Total radioactivity in urine and fecal samples was determined using a Packard Tri-Carb 2700 TR Liquid Scintillation Analyzer (PerkinElmer Life and Analytical Sciences, Boston, MA). The urine samples were prepared for scintillation counting by adding 100-μl aliquots to 10 ml of Ultima Gold scintillation fluid (PerkinElmer Life and Analytical Sciences). Each sample was counted for 10 min, and ^{14}C disintegration per minute was determined using a quenching curve. Feces samples were prepared for scintillation counting by making a suspension in water before transferring 1-ml aliquots (weighed) to absorbing pads. The sample aliquots were allowed to dry prior to combustion in a model 307 Packard Sample Oxidizer (PerkinElmer Life and Analytical Sciences). To aid the combustion, 100 μl of Combustaid (PerkinElmer Life and Analytical Sciences) was added to each sample prior to burning in the sample oxidizer. The combustion time was 1.25 min per sample, using solvent volumes of 10 ml of Carbo-Sorb E and 10 ml of Permafluor E+ (PerkinElmer Life and Analytical Sciences). The resulting "ready for scintil-

lation counting" samples were counted as described for the urine samples. The recovery from the sample oxidizer was found to be 99.6 ± 1.3% ($n = 7$). Spiking of a feces samples followed by combustion and counting of the samples showed a recovery of 97.7 ± 0.9% and a precision of 1.0% relative standard deviation.

Metabolite Profiling Using HPLC with Radiochemical Detection. Metabolite profiling in blood and urine was performed using HPLC with radiochemical detection following injection of approximately 4.0 mg of NC100668/kg (mixture of [Asn-U-^{14}C]NC100668 and NC100668) in three rats; the radioactive dose was approximately 17 MBq/kg. Blood samples (1 ml) were collected at 6 and 22 min postinjection from one rat and at 10 and 37 min postinjection from another rat; urine was collected up to 5 h after injection from the third rat.

The HPLC system consisted of a SP8800 ternary pump and SP8500 dynamic mixer (Thermo Electron Corporation, Waltham, MA) and a Gilson 231 (ASTED XL used without ASTED function) for an automatic sample injection (Gilson Medical Electronics, Villiers-le-Bel, France) equipped with a Rheodyne 7010 injection valve (Rheodyne Inc., Cotati, CA) and 10-μl injection loop. The column used was Supelcosil ABZ+Plus, 5 μm, 250 × 2.1 mm with a guard column Supelcosil ABZ+Plus, 20 × 2.1 mm (Supelco, Bellefonte, PA). Mobile phase A was 0.12% (v/v) perchloric acid in water/acetonitrile (80:20; v/v), and mobile phase B was 0.12% (v/v) perchloric acid in water/acetonitrile (30:70; v/v). The gradient was 0 to 19% mobile phase B (10 min), 19 to 22% mobile phase B (15 min), and 22% mobile phase B (10 min) with an equilibration time of 65 min with 0% mobile phase B before injection of a new sample. The flow rate was 0.5 ml/min. The radiochemical detector was a Packard Radiomatic Flo-One β A140A with 250 μl of γ-C flow cell (PerkinElmer Life and Analytical Sciences). Standard ^{14}C setting was used with an update time of 1 s. The scintillation fluid was Packard Ultima-Flo M (PerkinElmer Life and Analytical Sciences), and the scintillation flow rate was 1.5 ml/min. A UV detector (Spectra FOCUS; Thermo Electron Corporation) with a 6-mm, 9-μl Kel-F LC flow cell was coupled in series with the

TABLE 2

QWBA data and excretion data following injection of [Lys-U-^{14}C]NC100668 in male rats

Data for all organs are given as micrograms of equivalent per gram, i.e. the data are corrected with the self-absorption coefficients. The recoveries from urine and feces as well as the calculated recoveries for the whole-body and the total recovery are given as %ID. N.P., not present in the images. The data collected for urine during the first period (0–6 h) are shown together with the data for the animal killed 7 h after dosing.

	5 Min	20 Min	1 H	4 H	7 H	24 H	3 Days	7 Days
Adrenal	0.99	1.10	0.91	0.85	0.72	0.84	0.67	0.29
Blood	1.32	0.46	0.29	0.31	0.26	0.32	0.32	0.26
Bone marrow	0.62	0.84	1.83	2.33	1.57	1.86	0.81	0.28
Bone mineral	0.17	0.21	0.25	0.24	0.19	0.07	0.10	0.10
Brain	0.03	0.08	0.17	0.15	0.12	0.20	0.17	0.13
Epididymis	0.48	N.P.	0.56	0.49	0.35	0.63	0.42	N.P.
Eye	0.06	0.22	0.09	0.11	0.06	0.12	0.13	0.07
Fat (brown)	0.57	0.28	0.26	N.P.	0.42	0.45	0.45	0.24
Fat (white)	0.36	0.12	0.10	0.08	0.10	0.11	0.08	0.04
Harderian gland	0.56	0.42	0.55	0.53	0.50	0.59	0.44	0.19
Heart muscle	0.83	0.46	0.48	0.40	0.35	0.43	0.44	0.30
Intestine (small)	0.51	0.43	0.73	1.35	0.95	0.99	0.53	0.15
Intestine (large)	0.72	0.44	0.46	0.52	0.34	0.45	0.34	0.19
Kidney	11.6	9.96	9.91	12.05	5.84	5.76	3.34	1.78
Liver	1.24	0.81	0.88	0.58	0.63	0.53	0.54	0.30
Lung	1.21	0.45	0.32	0.23	0.27	0.33	0.25	0.17
Muscle	0.27	0.18	0.32	0.31	0.26	0.38	0.40	0.32
Pancreas	0.67	1.75	4.46	2.44	0.89	0.70	0.52	0.24
Testes	0.19	0.19	0.22	0.22	0.18	0.28	0.24	0.17
Salivary gland	0.69	0.68	1.57	1.46	0.91	0.68	0.50	0.23
Seminal vesicles	0.69	0.43	2.52	1.31	1.52	1.16	2.28	0.88
Skin	0.47	0.57	0.47	0.46	0.34	0.40	0.44	0.36
Spinal cord	0.04	0.15	0.26	0.19	0.18	0.18	0.14	0.12
Spleen	0.54	0.60	0.88	1.04	0.73	1.07	0.60	0.32
Stomach	0.89	0.53	1.19	0.59	0.69	0.67	0.44	0.28
Stomach content	0.00	0.00	0.01	0.03	0.03	0.02	0.01	0.01
Thymus	0.29	0.37	0.81	0.85	0.83	1.01	0.92	0.39
Urine bladder	1.92	1.72	1.03	0.16	0.18	0.10	0.11	0.04
Recovery QWBA	106.6	97.4	101.3	101.1	81.9	90.5	79.3	57.4
Urine (mean ± S.D.; $n = 3$)					6.1 ± 0.8	7.3 ± 0.8	8.2 ± 0.8	8.9 ± 0.9
Feces (mean ± S.D.; $n = 3$)						1.1 ± 0.2	2.3 ± 0.3	3.4 ± 0.2
Total recovery					88.0	98.9	89.8	69.8

radiochemical detector, and single wavelength detection was performed at 205 nm.

Metabolite Identification Using LC-MS Analyses. Samples to be used for metabolite identification in urine were obtained following the injection of approximately 5.0 mg of NC100668/kg (three rats) or 0.5 mg of NC100668/kg (two rats); urine samples were collected 5 h before and 5 h after injection of the agent. All urine and blood samples were stored in a −20°C freezer until analyzed.

A Hewlett Packard Series HP1100 system (Agilent Technologies, Palo Alto, CA) was used with a Phenomenex Luna C18(2), 3.5 μm, 2.1 × 150 mm column (Phenomenex, Torrance, CA). Mobile phase A was 0.2% (v/v) TFA in water, and mobile phase B was 0.2% (v/v) TFA in acetonitrile. The gradient was starting at 5% mobile phase B, increasing to 100% B in 30 min, and then back to 5% B in 1 min. The flow rate was 0.2 ml/min, and the analysis was performed at room temperature (approximately 22°C). The total chromatographic run time was 31 min. The samples were kept at 4°C, and 10 μl was injected for each analysis.

The HPLC system was coupled on-line to a LCQ Classic ion-trap mass spectrometer (Thermo Electronic Corporation); the interface between the LC and the MS was electrospray ionization in positive mode. The ion source and ionoptic parameters were optimized with respect to the [M+H]$^+$ ion of NC100194.

In Vitro Stability and Protein Binding Studies Using [Asn-U-^{14}C]NC100668. In vitro stability studies were performed using blood from two healthy male volunteers and from outbred male BrlWistHam@Mol rats. One-hundred microliters of [Asn-U-^{14}C]NC100668 (3.7 MBq/ml) was added per 900 μl of the biological fluid (human whole blood, human plasma, human serum, rat plasma, and rat serum; sodium citrate used as anticoagulant) and incubated at 37°C for up to 5 h. At the end of incubation a volume of acetonitrile, an equivalent to half the volume of the sample was added. The contents were mixed well and kept in a refrigerator overnight for maximum precipitation of protein. The precipitate was removed by centrifugation for 20

min at 13,000g and 6°C, and the resulting supernatant was analyzed using HPLC with radiochemical detection (as described above). Some rat and human serum samples were added a protease inhibitor cocktail; 850 μl of serum was then incubated with 50 μl of the P8340 inhibitor solution for 15 min at 37°C before the radiolabeled substance was added.

Protein binding to human plasma was studied using a Dianorm equilibrium dialyzer (Diachema AG, Zürich, Switzerland) equipped with 1-ml cells and a high-permeability mol. wt. 10,000 cut-off cellulose membrane (Diachema AG). Dialysis was performed for 18 h at 37°C (initial experiments showed that it was necessary to dialyze overnight to obtain equilibrium in the system), and the radioactivity in each cell was determined using liquid scintillation counting.

Analysis of Chromatographic and Mass Spectrometry Data. The chromatographic data obtained using the radiochemical detector and UV detector were processed using Turbochrom Client Server version 6.1.1 from PerkinElmer Life and Analytical Sciences. Thermo Finnigan Xcalibur version 1.0 SR1 was used for sampling and integration of the LC-MS chromatograms. Statistical calculations and graphical presentation of the data were prepared by GraphPad Prism version 2.00 from GraphPad Software Inc (San Diego, CA). Statistical calculations were in addition performed by Microsoft Excel 97 SR-2, from Microsoft Inc. (Redmond, WA). Mass Frontier Software version 3.0 from Thermo Electron Corporation was used to simulate fragmentation pattern in the MS.

Results

In Vitro Stability and Protein Binding of [Asn-U-^{14}C]NC100668. The ^{14}C-Asn-labeled NC100668 was shown to be quite stable in human whole blood and plasma, since less than 6% was metabolized during the 5 h of incubation at 37°C. However, the substance was less stable in serum, since up to 32% of the substance was metabolized during the 5 h of incubation in this matrix. These
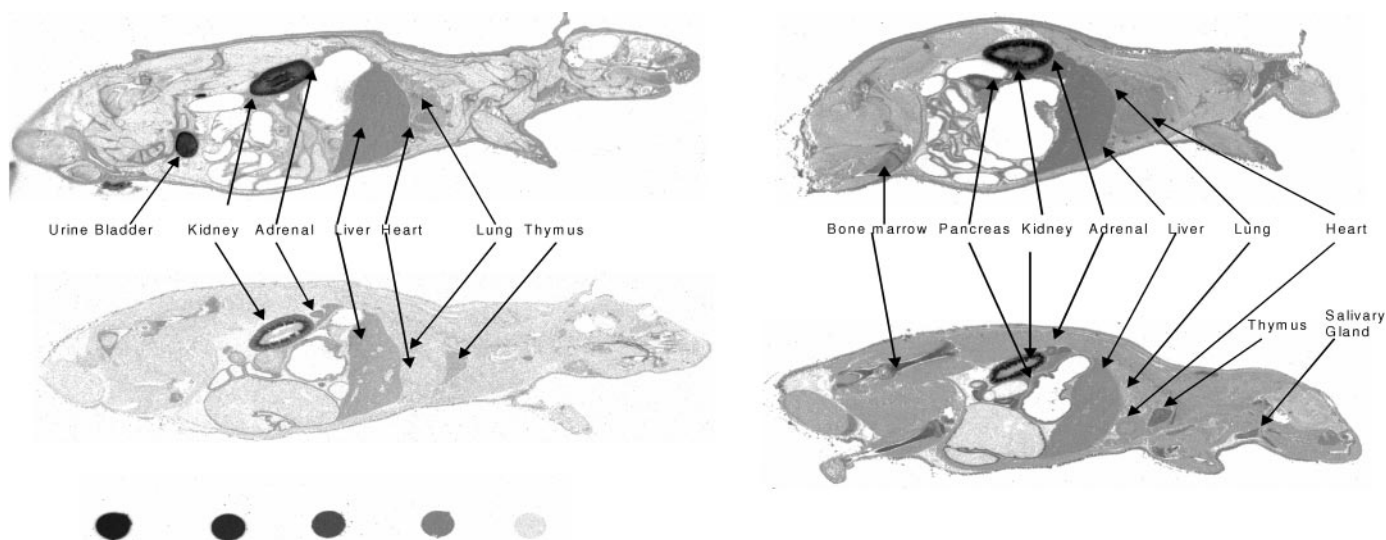
FIG. 2. Whole-body autoradiograms obtained after injection of [Asn-U-^{14}C]NC100668 (to the left) and [Lys-U-^{14}C]NC100668 (to the right). Top images at 20 min postdosing and bottom images at 24 h postdosing. The calibration standards contained approximately 75, 40, 15, 5, and 0.3 kBq/g.

results indicate that at least one protease activated during blood coagulation was involved in the reactions. [Asn-U-^{14}C]NC100668 was less stable in rat serum than in human serum, since approximately 56% was metabolized in rat serum during the 5 h of incubation. The difference between the two species was even larger for incubation in plasma, since approximately 45% of the substance was metabolized during the incubation in rat plasma. The difference observed between rat and human plasma might at least in part be caused by the high level of activation of coagulation factors often observed during blood sampling from rats. Experiments performed by adding a protease inhibitor cocktail to the incubation mixtures (data not shown) indicated that a major part of the in vitro metabolism was caused by protease(s).

Equilibrium dialysis experiments performed over a period of 18 h with human plasma showed that there was no significant protein binding of the ^{14}C-Asn-labeled substance ($0.4 \pm 0.9\%$; mean $\pm$ S.D.; $n = 6$). Control experiments showed that approximately 10% of the ^{14}C-Asn-labeled substance was metabolized during 18-h incubation in human plasma at 37°C.

Distribution and Excretion of [Asn-U-^{14}C]NC100668 Following Injection in Rat. The distribution of radioactivity in male rats obtained following injection of [Asn-U-^{14}C]NC100668 is detailed for all organs and all time points in Table 1; autoradiograms obtained 20 min and 24 h postdosing are shown in Fig. 2. The radioactivity was rapidly and evenly distributed throughout the body at 5 min postdosing, with the highest concentration in blood-rich organs such as adrenals, heart, kidney, liver, and lungs. The concentration of radioactivity was rapidly declining throughout the study period of 7 days, with the highest concentration in the kidneys. The data show a rapid urinary excretion with 62% ID (percentage of injected dose) excreted during the first 7 h. At 3 days postdosing, the total recovery of radioactivity was 89.6% ID with recoveries of whole-body section, urine, and feces comprising 17.4, 70.5, and 1.8% ID, respectively (Table 1). The highest concentrations of radioactivity in the body at 3 days were observed in blood-rich organs in addition to seminal vesicles, thymus, bone marrow, pancreas, and intestine wall. The autoradiograms of the kidney regions indicated a flow through the different regions with subsequent excretion and with small amounts retained and/or reabsorbed. Initially, the highest concentration in the kidney was seen in the medulla and outer cortex and rapidly declined in all regions

thereafter (Fig. 3A). No sex differences were observed in the overall distribution pattern (data not shown) or in the recovery data (a recovery of 16.4% ID was obtained 24 h after injection in the female rat).

Distribution and Excretion of [Lys-U-^{14}C]NC100668 Following Injection in Rat. The distribution of radioactivity in male rats obtained following injection of [Lys-U-^{14}C]NC100668 is detailed for all organs and all time points in Table 2; the autoradiograms obtained 20 min and 24 h postdosing are shown in Fig. 2. Like the ^{14}C-Asn-labeled substance, radioactivity was rapidly and evenly distributed in the body 5-min postinjection. However, the ^{14}C-Lys-labeled substance cleared much more slowly from the body than the ^{14}C-Asn-labeled substance, and the recoveries obtained for the whole-body section, urine, and feces at 3 days postinjection were 79.3, 8.2, and 2.3% ID, respectively, summing up to a recovery of 89.8% ID (Table 2). The highest amounts of radioactivity at this time point were observed in muscle (34.8% ID), skin (16.4% ID), kidney (7.5% ID), liver (5.4% ID), and blood (3.8% ID). The whole-body autoradiograms showed that following administration of [Lys-U-^{14}C]NC100668, the highest concentration of radioactivity was seen in kidney inner cortex (Fig. 2), indicating a reabsorption process; the time course for radioactivity in the kidney sections are shown in Fig. 3B. The autoradiogram obtained 24 h after injection (Fig. 2) shows uptake of radioactivity into bone marrow. No sex differences were observed in the overall distribution pattern (data not shown) or in the recovery data (a recovery of 85.3% ID was obtained 24 h after injection in the female rat).

Analyses of Blood and Urine Samples Following Injection of [Asn-U-^{14}C]NC100668 in Rat. The HPLC profiles of the four blood samples and the urine sample obtained following injection of the ^{14}C-Asn-labeled substance (i.e., labeling in the N-terminal amino acid) in rats are shown in Fig. 4. The peak with a retention time of approximately 24 min correspond to that obtained with [Asn-U-^{14}C]NC100668 (Fig. 4A). All chromatograms obtained with the blood samples (Fig. 4, B–E) were dominated by the parent compound corresponding to [Asn-U-^{14}C]NC100668 (Fig. 5A) and one metabolite peak with a retention time of approximately 2 min. In addition, some minor and less distinct peaks were observed at approximately 5.5, 16, and 20 min in the chromatograms for the samples obtained 6 min (Fig. 4B) and 10 min (Fig. 4C) after injection. These minute
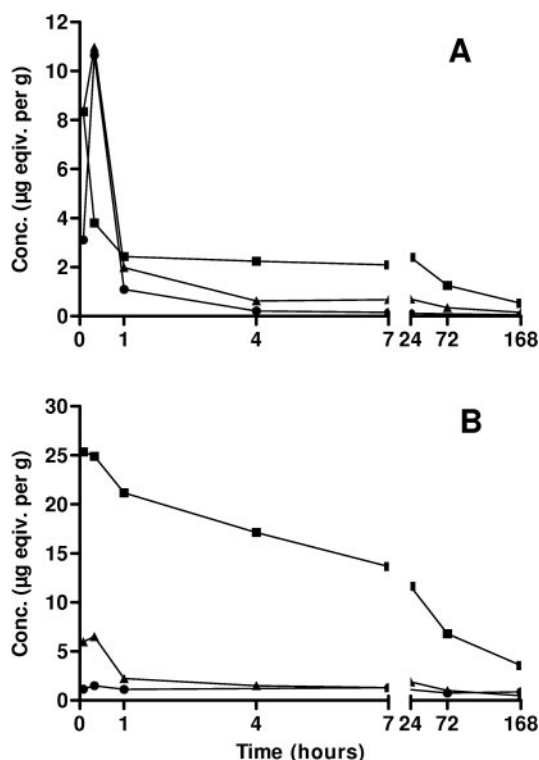
FIG. 3. Concentration of radioactivity in different kidney sections versus time following injection of [Asn-U-^{14}C]NC100668 (A) and [Lys-U-^{14}C]NC100668 (B); outer cortex (▲), inner cortex (■), and medulla (●). Note difference in scale.

peaks may in fact be noise only, and an accurate quantification of these peaks was not possible, but they were estimated to represent less than 8% of the total peak area. The parent compound/main metabolite ratios were estimated to be 80:20, 72:28, 40:60, and 18:82 at 6, 10, 22, and 37 min, respectively. Thus, the substance was rapidly metabolized, since more than half of the radioactivity present in blood was present in metabolites in the sample obtained 22 min after injection. It should be noted that a small change in retention was observed between the NC100668 standard (Fig. 4A) and the substance in blood (Fig. 4, B–E). This change in retention time was observed immediately upon mixing NC100668 with blood, plasma, or serum from either human or rat origin (data not shown). The reason for this small change in retention time is not known.

In urine, only one distinct chromatographic peak was observed (Fig. 4F), which showed a retention time of approximately 2 min (in void volume), i.e., similar to that of the main metabolite in blood. By changing the scale of the chromatogram to the level of visible baseline noise, only one minute single point "spike" constituting approximately 0.12% of the total peak area could be observed close to the retention time of the parent compound (Fig. 4G).

Identification of Metabolites in Rat Urine. Some initial analyses were performed on predose and postdose urine samples using the chromatographic conditions reported for quantification of NC100668 in plasma (Toft et al., 2005). These analyses, based on using a Waters Symmetry Shield RP8 column (Waters, Milford, MA), showed several differences in the MS spectra of predose and postdose samples at retention times very close to the void volume. The main signals observed in the postdose but not in the predose urine were at m/z values of 402.2 and 201.7, with somewhat less intense signals at m/z values of 232.3, 303.1, 345.1, 463.1, and 465.0 (data not shown). Because these signals were detected close to the void volume, i.e., in a region of the chromatogram where several
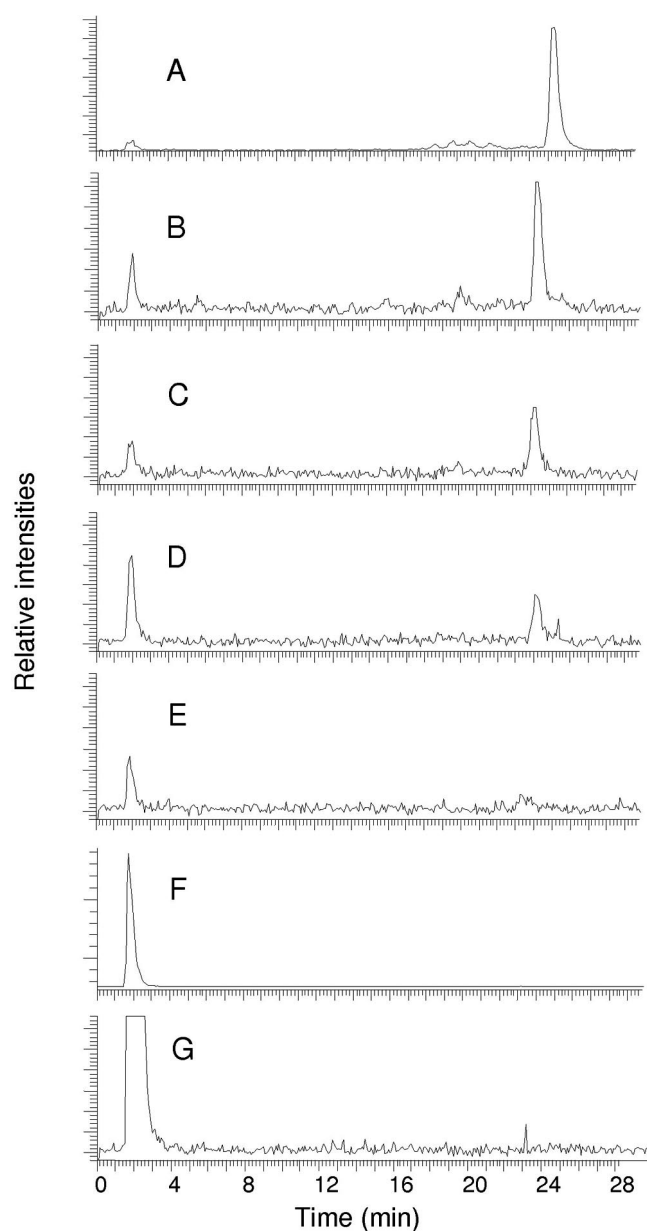

FIG. 4. HPLC chromatograms of blood (B, C, D, and E) and urine samples (F and G) obtained following injection of [Asn-U-^{14}C]NC100668 in rats compared with [Asn-U-^{14}C]NC100668 in saline (A). The chromatograms shown in B, C, D, and E were obtained using blood samples collected 6, 10, 22, and 37 min after injection, respectively; the response axes for B to E are normalized to the height of the major peak of chromatogram B. The chromatograms of rat urine sample obtained 5 h after injection of [Asn-U-^{14}C]NC100668 are shown both in full scale (F) and at a signal level, giving a baseline noise similar to that shown for the blood samples (G).

substances eluted, it was decided to look for another HPLC system to obtain retention of the substance(s) giving rise to these signals. The rest of the LC-MS data described were then obtained using the method with the Phenomenex Luna column described under *Materials and Methods*.

Using the method with the Luna column, differences between the predose and postdose urine samples were observed in the region with retention time of 11.60 to 12.00 min (chromatograms are shown as inserts in Fig. 5). As shown in Fig. 5, the major new MS signal observed in the postdose sample was at $m/z = 402.3$, whereas increased signals also were observed at m/z values of 201.8, 232.3, 244.3, 303.3, 343.5, 345.5, 463.1, 465.1, 591.1, and 648.1.
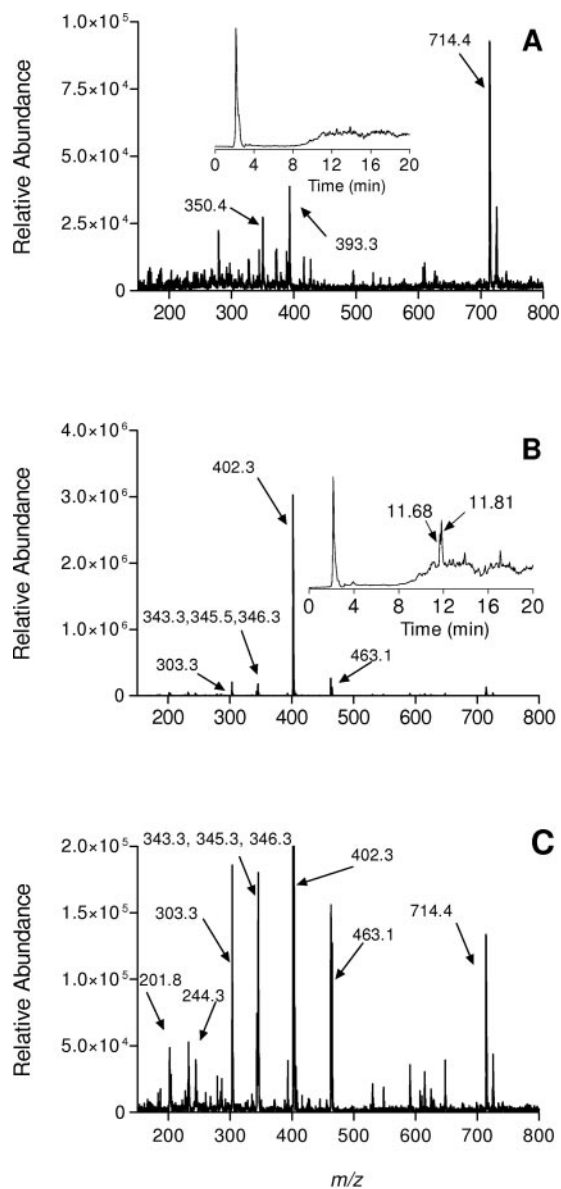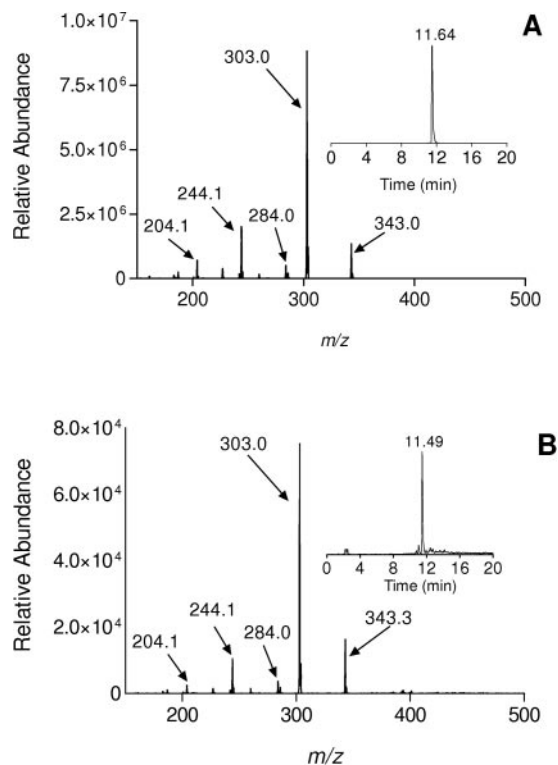
FIG. 6. The inserts show chromatograms based on MS/MS analysis. Product ion scan was performed at $m/z = 402.3 \pm 1.0$, and the total ion current chromatograms (mass range = 110 to 500) were recorded for Gly-NC100194 (A) and the postdose urine sample shown in Fig. 5 (B). MS/MS spectra (mass range, 150 to 500) of the main peaks were observed in the inserted chromatograms, i.e., following fragmentation in the MS of the ions giving rise to the signal at $m/z = 402.3 \pm 1.0$ of Gly-NC100194 (A) and the postdose urine sample (B).

FIG. 5. The inserts show the total current chromatograms (mass range, 150-2000) of rat urine samples predose (A) and following injection of 1.1 mg of NC100668 (B). The MS spectra (mass range, 150 to 800) were collected at the retention time of 11.60 to 12.00 min from the chromatograms shown in the inserts. Predose (A), postdose (B), and the postdose spectrum in B shown in an enlarged version (C).

Identification of C-Terminal Metabolites Gly-NC100194 and NC100194. It was hypothesized that the major signal at $m/z = 402.3$ could be due to the C-terminal fragment Gly-NC100194, and the signal at $m/z = 345.5$ could fit with NC100194. It was therefore decided to start the metabolite identification work by trying to identify the substances giving rise to these MS signals.

The chromatograms shown as inserts in Fig. 6 show that the substance in rat urine giving rise to the signal at $m/z = 402.3$ had a retention time similar to that of Gly-NC100194 (small variations were observed in the retention times obtained in different chromatograms with this substance). Moreover, MS/MS spectra (collision-induced dissociation of the $m/z = 402.3$ ion) resulted in exactly the same spectra for the metabolite in rat urine (Fig. 6B) and Gly-NC100194 (Fig. 6A). Thus, the main metabolite in urine was confirmed to be Gly-NC100194. Furthermore, these MS/MS spectra suggested that the signals observed in postdose urine samples at m/z values of 244.3,

303.3, and 343.5 could result from ion source fragmentation of this major metabolite in the MS. Finally, the small signal in postdose urine at $m/z = 201.8$ (Fig. 5C) was confirmed to be [Gly-NC100194 + 2H]$^{2+}$ based on the 0.5-mass unit spacing of isotopes typical for double charged ions (data not shown).

A proposal for the ion source fragmentation pattern of Gly-NC100194 is given in Fig. 7. This was obtained by simulating MS/MS fragmentation of Gly-NC100194 using the Mass Frontier Software. The simulated fragmentation (Fig. 7) gives m/z values exactly matching the experimentally obtained values (Fig. 6).

By performing experiments similar to that described above, it was shown that the substance in rat urine giving rise to the signal at $m/z = 345.5$ had a retention time and MS/MS spectrum similar to that obtained with pure NC100194 (data not shown). The main MS/MS fragments of this substance ($m/z = 187$, 246, and 286; data not shown) were all 57 units below those formed from Gly-NC100194 ($m/z = 244$, 303, and 343; Fig. 10A). As Gly contributes with a mass of 57, this means that the fragments formed from NC100194 were similar to those described for Gly-NC100194 in Fig. 7.

Further evidence for the interpretation of the m/z signals obtained from Gly-NC100194 and NC100194 is found in Fig. 8. This figure shows that the $m/z = 402.3$ ion chromatogram of the main metabolite cochromatographs and shows exactly the same peak split pattern as that observed for the ion chromatograms of $m/z = 343.3$, 303.3, and 201.8, thus confirming that the signals at $m/z = 343.3$, 303.3, and 201.8 represent fragmentation of Gly-NC100194 in the MS. On the other hand, the ion chromatogram of $m/z = 345.3$ shows a different pattern and a somewhat different retention time. Thus, although it is not known why this peak split pattern of Gly-NC100194 is obtained,
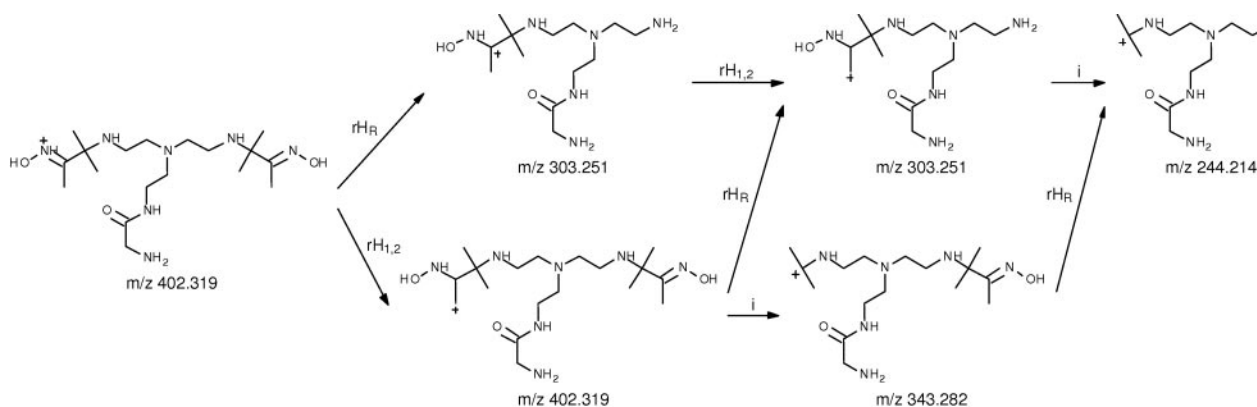
FIG. 7. A proposal for how Gly-NC100194 is fragmented in the MS, i.e., an explanation of the MS/MS spectra shown in Fig. 6.
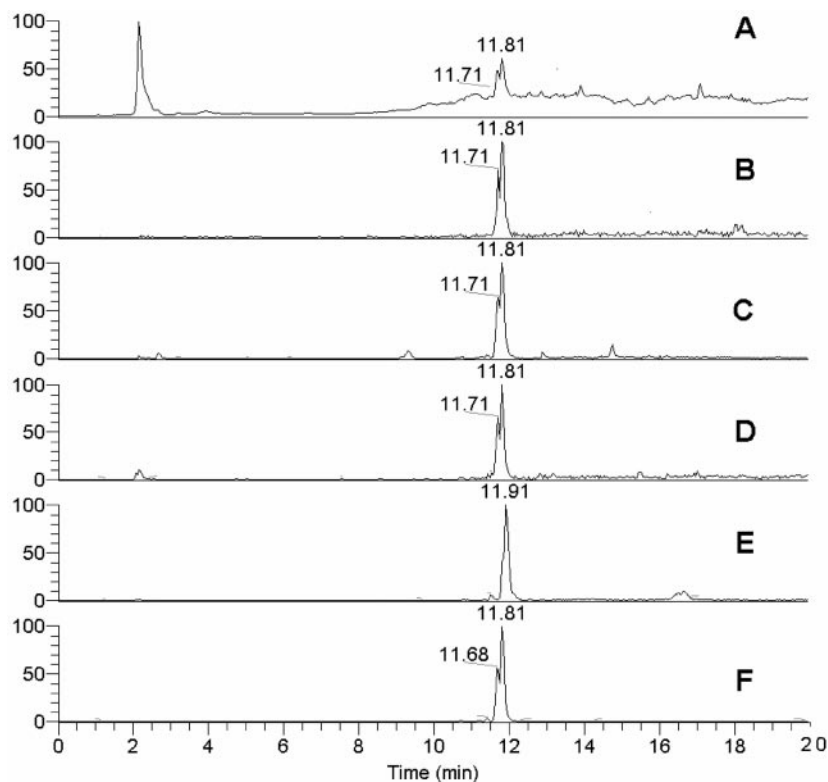

FIG. 8. The total ion current chromatogram (A) of the postdose urine sample shown in Fig. 4 is shown together with selected mass chromatograms (B–F) from the same data set. The selected mass chromatograms were obtained at m/z values of 201.8 ± 0.5 (B), 303.5 ± 0.5 (C), 343.3 ± 0.5 (D), 345.3 ± 0.5 (E), and 402.3 ± 0.5 (F).

the data clearly show that the signal at $m/z = 345.3$ is not caused by fragmentation of Gly-NC100194 in the MS but represent another metabolite with a very similar retention time, i.e., NC100194.

The MS signal intensity of the peak identified as NC100194 was in the range 1 to 14% of the signal intensity of the peak identified as Gly-NC100194 in the different urine samples. A similar ratio was observed in samples obtained from rats injected approximately 0.5 or 5.0 mg/kg NC100668. We tried to perform quantitative analyses of these two metabolites but were not able to obtain reliable data; we believe this problem to be due to the very high and varying concentration of low-molecular-weight substances in rat urine.

Work Performed Regarding Other MS Signals in Postdose Urine. Several theoretical metabolites that could be formed upon the splitting of peptide bonds of NC100668 have masses that fit with signals observed in the postdose but not in the predose urine sample (Fig. 5C). Thus, $m/z = 591.1$ fits with [Val-Ser-Pro-Tyr(3-iodo) + H]$^+$, $m/z =$

465.1 fits with [Val-Ser-Pro-Tyr + H]$^+$, $m/z = 463.1$ fits with [(Val-Ser-Pro-Tyr - 2H) + H]$^+$, $m/z = 232.3$ fits with [Val-Ser-Pro-Tyr + 2H]$^{2+}$, and $m/z = 303.3$ fits with [Acetyl-Asn-Gln + H]$^+$ in addition to being a possible degradation fragment (see above) of Gly-NC100194. No metabolite candidate was identified for the very weak signal observed at $m/z = 648.1$ (Fig. 5C).

To test whether these theoretical metabolites were real metabolites, Acetyl-Asn-Gln, Val-Ser-Pro-Tyr and Val-Ser-Pro-Tyr(3-iodo) were synthesized and shown to have different retention times or MS spectra from that observed in the postdose urine (data not shown). Thus, the signals observed at $m/z = 232.3$, 463.1, and 465.1 are not due to metabolites of NC100668, and the signal at $m/z = 303.3$ is due to a degradation fragment of Gly-NC100194 and not to the theoretical N-terminal metabolite Acetyl-Asn-Gln.

Attempts to Elucidate the Structure of an N-Terminal Metabolite. Experiments reported above with [Asn-U-^{14}C]NC100668 revealed
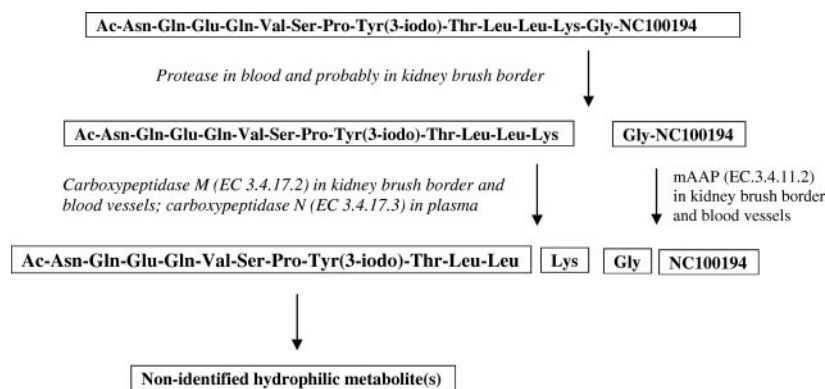
FIG. 9. Metabolic scheme for NC100668. Gly-NC100194 and NC100194 are excreted in urine; Lys is incorporated into protein metabolism. The structure of the N-terminal very hydrophilic metabolite is not identified, and it is not known what happens to the part of NC100668 that is on the N-terminal side of the Lys residue. The proteases most likely to be responsible for the metabolism of the agent are given; mAAP, membrane alanyl aminopeptidase.

only one very early eluting radioactive metabolite peak from this N-terminal amino acid of NC100668. However, at the very early retention time for this metabolite, we did not succeed in finding any distinct additional MS signals in the postdose urine sample compared with the predose sample. A further attempt to elucidate the structure of this N-terminal metabolite was performed by injecting an equal mixture of [Asn-U-^{14}C]NC100668 and NC100668 in a rat. Thus, one should expect to find two MS signals (or two sets of MS signals) of similar intensity in the urine of this rat; i.e., the signal from the radioactive metabolites should be 8 m/z units higher than for the nonradioactive form of the metabolites reflecting the four labeled carbon atoms. Even this effort did not reveal any characteristic signals that could indicate the masses of an N-terminal metabolite in the urine.

Discussion

NC100668 is rapidly metabolized following injection in rats as more than half of the radioactivity in blood was recovered in one metabolite peak 22 min after injection of [Asn-U-^{14}C]NC100668, i.e., labeling of the N-terminal amino acid. Only one radioactive peak with a retention time similar to the radioactive N-terminal metabolite in blood was detected in urine; i.e., the parent substance was not observed in urine. Further evidence for the rapid metabolism of this agent comes from LC-MS analysis of intact and unlabeled NC100668 in toxicokinetic studies, which showed that the total clearance of NC100668 both in rats and dogs were approximately twice the literature values for glomerular filtration rates. Thus, toxicokinetic studies (data not shown) with a dose range of 100 to 1000 μg/kg NC100668 in rats showed a mean total clearance value of 18.4 ml/min · kg, whereas the renal filtration rate in rats is 8.0 ml/min · kg (Renkin and Gilmore, 1973); studies with a dose range of 25 to 250 μg/kg in dogs showed a mean clearance value of 8.4 ml/min · kg, whereas the renal filtration rate in this species is 4.3 ml/min · kg (Renkin and Gilmore, 1973).

The retention time of the N-terminal metabolite observed in urine following injection of [Asn-U-^{14}C]NC100668 indicates that this metabolite is very hydrophilic (or several metabolites with a similar hydrophilicity). Identification of the metabolite(s) was complicated by the presence of large amounts of low-molecular-mass signals, originating from endogenous amino acids, peptides, and other low-molecular-weight substances in rat urine. Even the effort to inject a mixture with equal amounts of [Asn-U-^{14}C]NC100668 and NC100668, which should give two MS signals of similar intensity with 8 m/z units difference, did not reveal any characteristic signals reflecting any distinct N-terminal metabolite(s) in the urine. The N-terminal radio-

labeled metabolite peak may contain just Acetyl-Asn, Asn, some short peptide fragment, or deamidated forms of these substances, or it may contain a mixture of some of these substances. Due to the fact that many such possible structures exist for the N-terminal metabolite(s) (note that the N-terminal tetrapeptide contains three acid amide groups), we decided not to develop an alternative chromatographic method to try to identify the metabolite(s) by cochromatography with reference substances.

Two C-terminal metabolites were identified in the rat urine samples; Gly-NC100194 was the dominant metabolite with minor amounts of NC100194 (1–14% relative to Gly-NC100194). No other metabolites were identified. The observation that Gly-NC100194 was the major C-terminal metabolite and NC100194 a minor C-terminal metabolite in rat urine fits well with data obtained with ^{99m}Tc-NC100668, since urine samples obtained following the injection of the ^{99m}Tc-labeled substance contained a single radioactive peak, which cochromatographed with ^{99m}Tc-labeled Gly-NC100194 (D. Edwards, personal communication). Thus, NC100668 seems to be metabolized the same way independent of any Tc-binding to the chelate. Overall, it seems that the peptide part of the agent is almost completely degraded, although the present study does not reveal what happens in detail to the part of NC100668 on the N-terminal side of the Lys residue (see metabolic scheme in Fig. 9).

There are many proteases in the body that are able to cleave peptides/proteins at the C-terminal side of Lys (and Arg) residues. Whereas the pancreatic enzyme trypsin (EC 3.4.21.4) cleaves at these sites without being specific to the surrounding amino acid sequences, most other proteases cleaving C-terminal to Lys are more specific concerning the surrounding amino acid sequence. This is the case for many proteases involved in different physiological processes such as those involved in blood coagulation, fibrinolysis, the complement activation system, and processing of protein hormone precursors. In addition to these proteins circulating in blood, proteases bound to blood cells and endothelial cells within blood vessels might also be involved in the metabolism of NC100668. Furthermore, one or more of the many matrix proteases might also be involved in this metabolism. Thus, there are many proteases with the ability to cleave Gly-NC100194 from NC100668 before the substance enters the kidneys. Within the kidneys, a "trypsin-like protease" present in large amount in the brush-border membrane (Guder and Ross, 1984) is an obvious candidate for cleaving Gly-NC100194 from NC100668.

Based on the present data, it is not possible to conclude whether most of Gly-NC100194 is formed in blood or in the kidneys. The presence of both NC100668 and Gly-NC100194 in blood together with the observation that there is no NC100668 present in urine,

despite being present in blood for more than 1 h (blood kinetic data not shown), makes it very likely that Gly-NC100194 is formed partially in blood and partially at the kidney brush-border membrane, with probably most of the metabolite being formed within the kidneys.

The NC100194 observed in rat urine is most likely formed by attack of an aminopeptidase on Gly-NC100194. The membrane alanyl aminopeptidase (EC 3.4.11.2), which is present in large amounts on the kidney brush-border membrane (Turner, 1998), is a very likely candidate for removing Gly from Gly-NC100194. This enzyme is also present on the apical side of endothelial cells in blood vessels (Turner, 1998) and thus may be responsible for formation of some small amounts of NC100194 already in blood.

The QWBA studies using [Lys-U-^{14}C]NC100668 revealed the highest concentration of radioactivity in renal inner cortex, suggesting that the Lys residue is reabsorbed in the tubules and then enters into protein metabolism. The rationale for this fate of the Lys residue is most likely due to a carboxypeptidase releasing the C-terminal Lys formed after cleavage of Gly-NC100194 from NC100668. There are many carboxypeptidases in the body that are able to remove C-terminal Lys. Indeed, many proteases used to activate physiological processes act by cleaving peptides/proteins at the C terminus of Lys/Arg. Moreover, to preserve balance in the body, carboxypeptidases able to remove the C-terminal Lys/Arg inactivate such newly formed active peptides/proteins. The most likely enzyme to release the C-terminal Lys from the metabolite formed following release of Gly-NC100194 is carboxypeptidase M (EC 3.4.17.2), which is present both on the kidney brush-border membrane and on endothelial cells within blood vessels (Skidgel, 1998). Another candidate to remove this C-terminal Lys is the lysine carboxypeptidase (also called carboxypeptidase N; EC 3.4.17.3), which is active in plasma (Skidgel and Erdös, 1998).

In conclusion, NC100668 is rapidly metabolized in rats. The radiolabeled N-terminal amino acid is mainly excreted in urine, whereas the radiolabeled Lys close to the C-terminal end is mostly incorporated into protein metabolism. Two metabolites from the C-terminal end containing the Tc-binding chelator were identified in urine with approximately 10 times as much Gly-NC100194 as NC100194.

References

Guder WG and Ross BD (1984) Enzyme distribution along the nephron. *Kidney Int* **26:**101–111.

Ichinose A, Tamaki T, and Aoki N (1983) Factor XIII-mediated cross-linking of NH$_2$-terminal peptide of α$_2$-plasmin inhibitor to fibrin. *FEBS Lett* **155:**369–371.

Jaffer FA, Tung C-H, Wykrzykowska JJ, Ho N-H, Houng AK, Reed GL, and Weissleder R (2004) Molecular imaging of factor XIIIa activity in thrombosis using a novel, near-infrared fluorescent contrast agent that covalently links to thrombi. *Circulation* **110:**170–176.

Lee KN, Lee CS, Tae W-C, Jackson KW, Christiansen VJ, and McKee PA (2001) Crosslinking of α$_2$-antiplasmin to fibrin. *Ann NY Acad Sci* **936:**335–339.

Lijnen HR, Holmes WE, van Hoef B, Wiman B, Rodriguez H, and Collen D (1987) Amino-acid sequence of human α$_2$-antiplasmin. *Eur J Biochem* **166:**565–574.

Liu S, Edwards DS, and Barrett J (1997) ^{99m}Tc labeling of highly potent small peptides. *Bioconjug Chem* **8:**621–636.

Moroi M and Aoki N (1976) Isolation and characterization of α$_2$-plasmin inhibitor from human plasma. *J Biol Chem* **251:**5956–5965.

Renkin EM and Gilmore JP (1973) Glomerular filtration, in *Handbook of Physiology—Renal Physiology* (Orlogg J and Berliner RW eds) pp 185–248, Williams & Wilkens, Baltimore, MD.

Silverstein MD, Heit JA, Mohr DN, Petterson TM, O'Fallon WM, and Melton LJ (1998) Trends in the incidence of deep vein thrombosis and pulmonary embolism. *Arch Intern Med* **158:** 585–593.

Skidgel RA (1998) Carboxypeptidase M, in *Handbook of Proteolytic Enzymes* (Barret AJ, Rawlings ND, and Woessner JF eds) pp 1347–1349, Academic Press, San Diego.

Skidgel RA and Erdös EG (1998) Lysine carboxypeptidase, in *Handbook of Proteolytic Enzymes* (Barret AJ, Rawlings ND, and Woessner JF eds) pp 1344–1347, Academic Press, San Diego.

Toft KG, Oulie I, and Skotland T (2005) Quantification of NC100668, a new tracer for imaging of venous thromboembolism, in human plasma using reversed-phase liquid chromatography with electrospray ion-trap mass spectrometry. *J Chromatogr B*, in press.

Turner AJ (1998) Membrane alanyl aminopeptidase, in *Handbook of Proteolytic Enzymes* (Barret AJ, Rawlings ND, and Woessner JF eds) pp 996–1000, Academic Press, San Diego.

Ullberg S (1977) The technique of whole-body autoradiography-cryosectioning of large specimens, in *Scientific Tools, the LKB Instrument Journal* special issue, pp 2–29, LKB Instrument Inc, Gaithersburg, MD.

Address correspondence to: Dr. Tore Skotland, Research and Development, GE Healthcare Bio-Sciences, Nycoveien 2, N-0401 Oslo, Norway. E-mail: tore.skotland@ge.com